Experimental investigation of high-frequency-difference twin beams in hot cesium atoms

Miaojun Guo, Haitao Zhou, Dan Wang, Jiangrui Gao, Junxiang Zhang,* and Shiyao Zhu
The State Key Laboratory of Quantum Optics and Quantum Optics Devices, Institute of Opto-electronics, Shanxi University, Taiyuan 030006, People's Republic of China
(Received 22 September 2013; published 10 March 2014)

We experimentally investigate the quantum-correlated twin beams generated through stimulated nondegenerate four-wave mixing in the double-lambda atomic system. A 2.5-dB noise reduction of intensity difference with 18.4-GHz frequency difference at the cesium D_1 line is observed in a Cs vapor cell. The quantitative theoretical analysis reveals the experimental difficulty in getting high quantum correlation in Cs atoms because of the large hyperfine splitting of the ground states. However, it is favorable for obtaining quantum correlation in a wide range of pump detunings and relative long lengths of vapor cells. This quantum correlation provides a potential resource for possible coherent interfaces between atomic and solid-state systems due to its wavelength at the Cs D_1 line which lies well within the wavelength regime of the exciton emission from InAs quantum dots.

DOI: 10.1103/PhysRevA.89.033813 PACS number(s): 42.50.Gy, 42.50.Ct, 42.50.Lc, 42.65.Lm

I. INTRODUCTION

The quantum-correlated twin beams with continuous variables is an important quantum resource for developing practical quantum information protocols from finite to infinite dimensions [1]. Because of its high intensity (bright in contrast to the vacuum squeezed states) [2], it can be relatively easily detected by direct detection [3] and used for many applications, such as sub-shot-noise measurement [3,4], high-sensitivity spectroscopy [2], and secure quantum communication and quantum imaging [1,5–10]. The most well-known quantum resources are generated from continuous-wave nondegenerate optical parametric oscillators (cw-NOPOs) operating above threshold [2–4,11,12]. However, NOPOs are normally operated at a frequency far detuned from the atomic transition frequency, which limits the realization of atom-based quantum communication protocols, where the wavelength of correlated fields is required to match the atomic transition [13–15]. Thereafter, the direct generation of correlated photon pairs for discrete variables in atomic ensembles was first proposed [16], and the experimental investigations of discrete correlated photon pairs were carried out in double-lambda systems of Rb [17,18] and Cs [19] cold atoms.

Based on the experimental and theoretical studies, the quantum coherence of electromagnetically induced transparency (EIT) [20] is a successful technique which can result in the enhancement of nonlinear processes in atomic systems [21–24]. The combination of the EIT and the four-wave mixing (FWM) therefore opened the way to generation of bright continuous-variable correlated twin beams at atomic transition wavelength [25], and the further developments of this kind of twin beam were performed in a Rb vapor cell [8,9,26–30] and sodium atoms [31]; the theoretical explanation was also provided based upon the process of FWM [32,33]. These measurements and theories seemed to be in agreement with, but lacked the precision needed to discriminate between different atomic systems of Rb and other atoms, e.g., Cs, in which the twin beams have not been produced. In this paper, we not only demonstrated the observation of twin beams in Cs atoms, but also pinpointed the difference in obtaining the correlation in different atoms. Therefore the dependence of quantum correlation on the concrete parameters of atoms was explored. Furthermore, the improvement by taking high single-photon detuning and the long length of the cell was made to establish the quantum correlation in Cs atoms. These quantum-correlated light fields at the wavelength of the Cs atomic transition may be of particular importance for the quantum integrated light–atomic ensemble interface in long-distance quantum communication networks [16], because Cs atoms can provide several advantages: Their hyperfine splitting of ground states is specialized for the clock transition allowing the realization of all-optical atomic clocks [34], and their D_1 line at 894 nm lies well within the wavelength regime of the exciton emission from InAs quantum dots [35] for possible coherent interfaces between atomic and solid-state systems [36]. We believe that the obtained results would be useful for implementation of quantum computation and quantum information processing with atomic and solid-state systems.

II. EXPERIMENTAL SETUP

The D_1 line of Cs atoms is used to form a double-Λ-type three-level system with an upper level $|3\rangle$ ($6\,^2P_{1/2}, F' = 4$) and two lower levels $|1\rangle$ and $|2\rangle$ ($6\,^2S_{1/2}, F = 4$ and $6\,^2S_{1/2}, F = 3$) [see Fig. 1(a)]. The frequency difference between the two lower levels is $\delta = 9.2$ GHz. The decay rate of the upper level is $\Gamma = 2\pi \times 4.6$ MHz. The two transitions from $|3\rangle$ to $|1\rangle$ and $|2\rangle$ are simultaneously driven by a strong pump field (frequency ω_0) with different single-photon detunings $\Delta + \delta$ and Δ. The transition $|3\rangle \leftrightarrow |1\rangle$ is also coupled with a weak probe field (ω_a) with detuning Δ. Therefore a high-efficiency FWM process is obtained due to Raman-driven coherence between the two lower levels in the double-Λ-type three-level scheme (see Eqs. (3) and (4) in Ref. [37]). When two pump lights are simultaneously absorbed, the probe light is amplified by a stimulated Raman nondegenerate FWM process, while the conjugate light with frequency $\omega_b = 2\omega_0 - \omega_a = \omega_a + 2\delta$ is generated under two two-photon resonance (one for pump and probe lights, and the other for pump and the conjugate lights) and phase-matching conditions; hence the quantum correlation

*junxiang@sxu.edu.cn

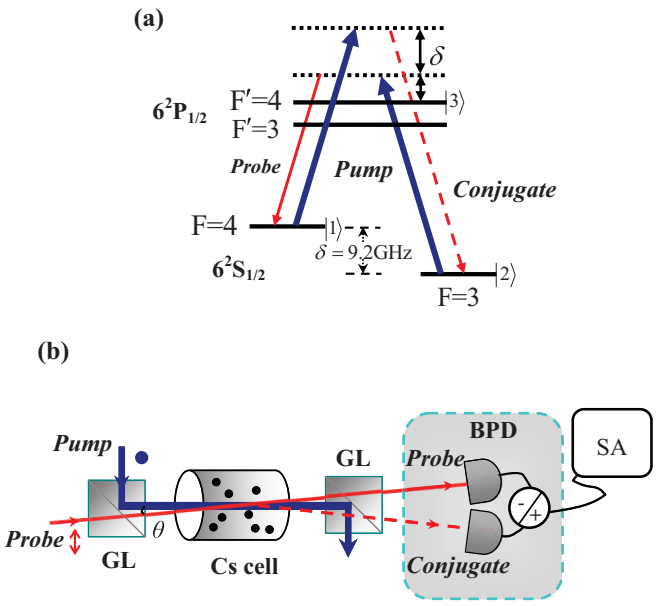

FIG. 1. (Color online) (a) Relevant levels of the ^{133}Cs D_1 line showing a double-lambda system. (b) Experimental setup. GL: Glan-laser polarizer; BPD: balanced photo detector; SA: spectrum analyzer.

is established between the probe and conjugate lights with 18.4 GHz frequency difference. In the experiment, we use two independent Ti:sapphire lasers with narrow linewidth (~40 kHz) for the pump and the probe fields; the frequencies are locked via their interlock controller systems, respectively. We determined that the diode laser cannot be used as probe or pump in our system, because its high phase noise will lead to phase-to-amplitude noise conversion due to atomic dispersion [38,39].

The experiment is performed in four ^{133}Cs vapor cells with the lengths of $L = 5$, 10, 15, and 25 mm at a temperature of 112 °C, and the losses of the far-off resonant light through the cells are on the order of 12% (for 5- and 10-mm cells) and 14% and 7% (for 15 and 25 mm). In order to realize the optimal overlap between incident probe and pump, the e^{-2} full widths of probe and pump are 0.5 and 0.67 mm, respectively. The probe light is incident into the cell at a small angle $\theta = 0.38°$ relative to the pump light; see Fig. 1(b). The correlation is measured with two balanced photo detectors (BPDs).

III. EXPERIMENTAL RESULTS

Now let us examine the quantum correlation between the probe and conjugate fields via measuring their intensity-difference noise reduction. We set the intensity of the pump and probe lights to 450 mW and 200 μW, and the single-photon detunings to $\Delta = 613$, 905, 1314, and 1634 MHz for the four vapor cell lengths $L = 5$, 10, 15, and 25 mm (see Fig. 2) to get optimum noise reduction, while the two-photon resonance condition is satisfied. For balanced homodyne detection, the noise levels of the photocurrents from the probe and conjugate lights are balanced by using variable gain amplifiers (VGA); see green and pink lines in Fig. 2 for analysis frequency from

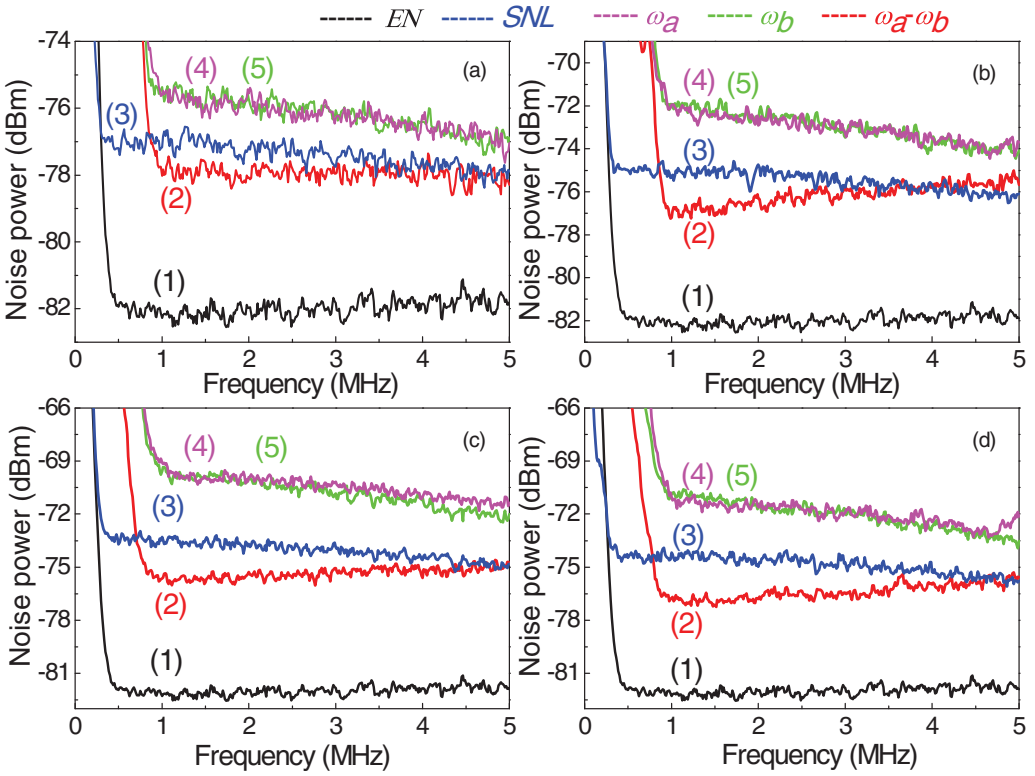

FIG. 2. (Color online) The intensity-difference noise power spectrum. (1) EN (black lines), (2) $\omega_a - \omega_b$ (red lines), (3) SNL (blue lines), (4) ω_a (pink lines), (5) ω_b (light green lines). (a) $L = 5$ mm, $\Delta = 613$ MHz; (b) $L = 10$ mm, $\Delta = 905$ MHz; (c) $L = 15$ mm, $\Delta = 1314$ MHz; (d) $L = 25$ mm, $\Delta = 1634$ MHz. The resolution bandwidth is 100 kHz, the video bandwidth is 100 Hz.

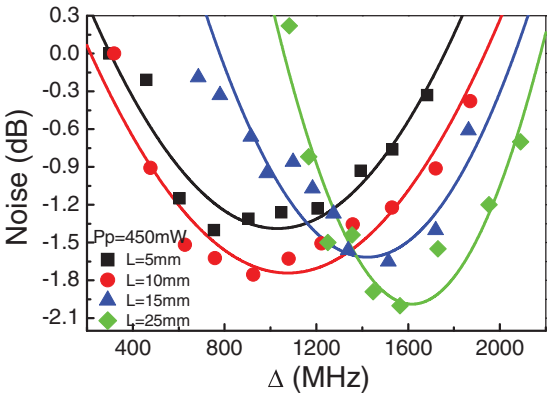

FIG. 3. (Color online) Intensity-difference noise vs Δ for different lengths of vapor cells with pump power 450 mW and probe power 200 μW. The solid lines are the fitted lines to data points.

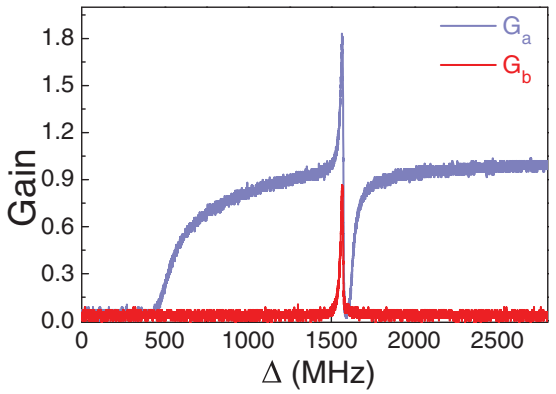

FIG. 4. (Color online) The gain of probe (light blue line) and conjugate (red line) lights. The main experimental parameters are $\Delta = 1565$ MHz, $P_p = 450$ mW, $P_{\rm pr} = 200$ μW, $L = 25$ mm, $\theta = 0.38°$, $T = 112$ °C.

0 to 5 MHz. In some cases the two curves are inconsistent with each other as shown in Figs. 2(c) and 2(d), making it difficult to balance the noises in a wide range of analysis frequency. The twin beams with the maximum intensity-difference noise reductions [see red lines in Figs. 2(a)–2(d)] below the shot-noise levels (SNLs) of 1, 2, 2.1, and 2.5 dB (for $L = 5$, 10, 15, and 25 mm) are obtained. The SNL [blue lines in Figs. 2(a)–2(d)] is calibrated by illuminating the two detectors with two Ti:sapphire laser beams. Consequently, the corresponding intensity-difference noise squeezing would be -1.2, -2.4, -2.5, and -3.2 dB if the measured squeezings are corrected from the electronic noise (black lines). Here we would like to emphasize that the maximum noise reductions are observed at different single-photon detunings (Δ) in different cells, in which the twin beams are generated with different power, leading to the different noise power of SNL being calibrated for each measurement.

In order to investigate the underlying mechanism of the dependence of noise reduction on the parameters of the system, especially the single-photon detuning, we show in Fig. 3(a) a series of intensity-difference noise spectra vs detuning Δ for the different lengths of vapor cells (four colored lines in Fig. 3). The measured noise reduction shows a dip structure. There exists an optimum detuning Δ where we have the maximum noise reduction for a concrete vapor cell. This detuning-dependent correlation can be understood in terms of a stimulated Raman gain FWM process in atomic medium. For a given FWM system with the gain G (defined as the ratio of an amplified probe power to an input probe power), the intensity-difference noise, expressed in dB relative to the standard quantum limit(SQL), has the predication formula $10\log_{10}[1/(2G-1)]$ [27]. Therefore the higher gain results in larger intensity-difference noise reduction. The dependences of the gain (which is evaluated as the value of the photon current at the two-photon gain peak over the far-detuned photon current when the probe is scanned across the two-photon resonance; see Fig. 4) and quantum correlation on pump detuning under two-photon resonance are depicted in Fig. 5. In Fig. 4, the dispersionlike gain spectrum of the probe field (light blue line for $G = G_a$) gives both Raman FWM gain peak and Raman absorption dip [31], and the conjugated gain is generated when Raman FWM occurs (red line for $G_b = G - 1$). The gain first increases with the increase of detuning, leading to the increase of quantum correlation; see Figs. 5(a) and 5(b). However, in our system, there is an additional noise from the spontaneous emission of the atoms; it enters the generated fields through the Langevin noise especially for small detuning Δ. Therefore, the quantum correlation vanishes at small detuning [see Figs. 5(c) and 5(d)]. Due to the balance between the gain-resultant noise reduction and added Langevin noise, there is a maximum noise reduction at a certain detuning depending on other parameters. The quantum correlation can be observed in a wider range of detuning from 300 MHz to 2.1 GHz (see Fig. 5), yielding the quantum-correlated twin fields in a wider frequency region. Notice that, in Fig. 5, the measured correlations (blue solid triangles) are lower than the values estimated from the formula $10\log_{10}\{[\eta + (1-\eta)(2G-1)]/(2G-1)\}$ (blue hollow triangles in Fig. 5) with the total detection efficiency $\eta = 78.5\%$, including the quantum efficiency of the photodetectors (87% for 895 nm), the transmission efficiency through the vapor cell's window (93%), and the collector efficiency (estimated as 97%).

Besides, it is seen that the best quantum correlation is obtained with long cell length and large Δ. The increase of the cell length results in the increase of both the Langevin noise and the two-photon gain, which leads to the large quantum correlation if the Langevin noise is suppressed at large detuning regime. In addition, there exist complex effects including the Langevin noise, the gain saturation, and pump depletion, for which the gain of the generated conjugate field is larger than that of the probe [40] (on the left side of dashed lines in Figs. 5(c) and 5(d).

IV. THEORETICAL DISCUSSION

The effective Hamiltonian that describes the Raman-driven FWM process ($\hbar = 1$) is [41]

$$\hat{H}_{\rm eff} \approx i\chi\hat{a}^{+}\hat{b}^{+} - i\chi^{*}\hat{a}\hat{b}, \tag{1}$$

where $\chi = N\Omega^2 g_{31}^{*} g_{32}^{*} \frac{4(\delta-2\Delta)[(\delta^2-6\delta\Delta+6\Delta^2)+(\delta-\Delta)^2(\Delta^2+\gamma^2)/\Omega^2]}{(\delta^2-2\delta\Delta+2\Delta^2)^3}$. N is the number of atoms, Ω represents the Rabi frequency of

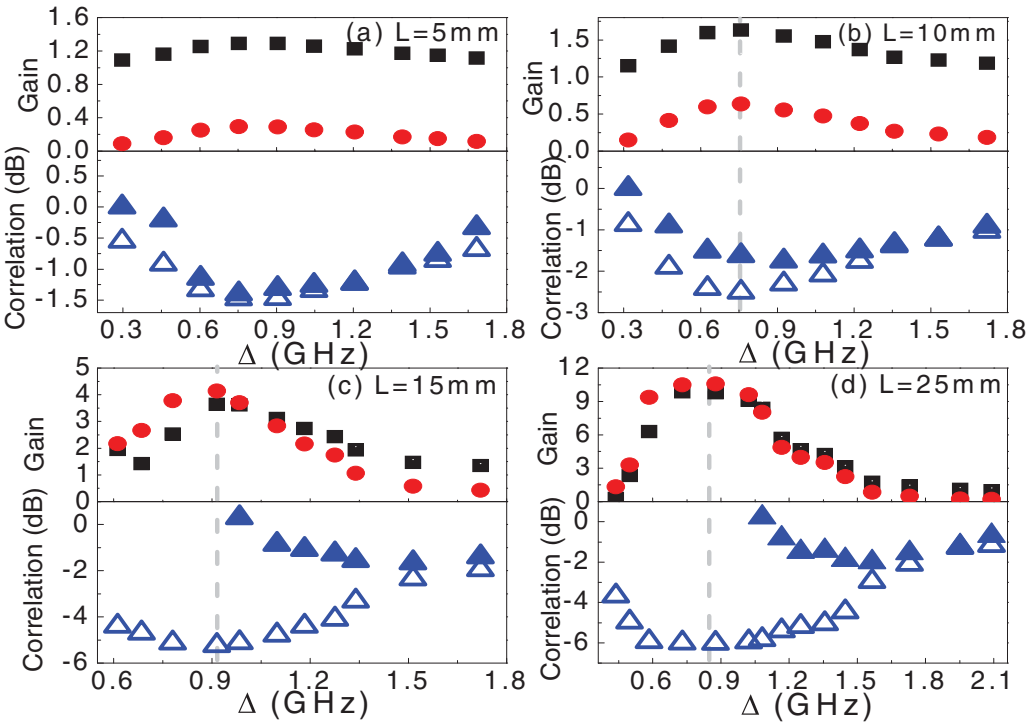

FIG. 5. (Color online) The measured gains of output probe (black squares) and conjugate (red circles) beams, as well as the measured (blue solid triangles) and predicated (blue hollow triangles) intensity-difference correlation: (a) $L = 5$ mm, (b) $L = 10$ mm, (c) $L = 15$ mm, (d) $L = 25$ mm. The pump power is 450 mW; the other parameters are the same as in Fig. 3.

the pump, and g_{31} (or g_{32}) is the atom-field coupling constant between the atom and probe field denoted by the annihilation operator $\hat{a}$ (or the conjugate field $\hat{b}$).

In Eq. (1), we keep only the phase-matching terms and drop the constant terms. Set $\gamma/\delta \approx 0$, $|\Omega/\delta|^2 \approx 0$, $|\Delta\Omega/\delta^2| \approx 0$ because of the large δ (several GHz, e.g., 9.2 GHz for ^{133}Cs, 3.0 or 6.8 GHz for ^{85}Rb or ^{87}Rb) and small decay rate γ (several MHz). In this experiment, Ω is about several hundred MHz and Δ is 300 MHz $-$ 2 GHz. It is easy to see from Eq. (1) that the quantum correlation between $\hat{a}$ and $\hat{b}$ is established via the FWM process, where the third-order nonlinear susceptibility χ has a dependency on atomic parameters. Using the input-output relations—$\hat{a}_{\rm out} = \sqrt{G}\hat{a}_{\rm in} + \sqrt{G-1}\hat{b}^{+}_{\rm in}, \hat{b}_{\rm out} = \sqrt{G}\hat{b}_{\rm in} + \sqrt{G-1}\hat{a}^{+}_{\rm in}$, where $\hat{a}_{\rm out}(\hat{b}_{\rm out})$, $\hat{a}_{\rm in}(\hat{b}_{\rm in})$ are the annihilation operators for output and input probe (conjugate) fields after an interaction time t in atoms—we obtain $G = \cosh^2 \chi t$ and $G - 1 = \sinh^2(\chi t)$, the gains of the probe and conjugate fields, respectively. If we consider the inevitable experimental detection losses, modeled by an approximation of a beam splitter efficiency η, the degrees of intensity-difference squeezing are reduced to $10\log_{10}\{[\eta + (1-\eta)(2G-1)]/(2G-1)\}$.

The predicted Raman gain (solid lines) and intensity-difference squeezing (dashed lines) vs detuning Δ and interaction time t are shown in Fig. 6 for two cases of ^{133}Cs (thick red lines) and ^{87}Rb (thin blue lines), the dashed lines

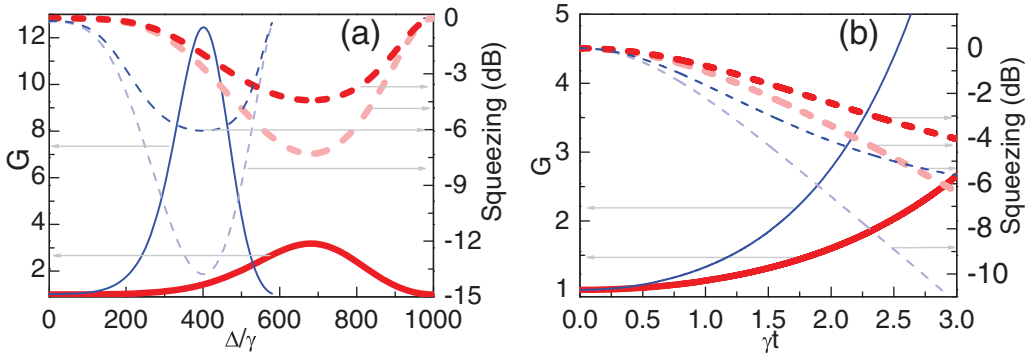

FIG. 6. (Color online) The gain G (solid lines) and intensity-difference noise squeezing (dashed lines) as the function of the detuning Δ (a) and the interaction time t (b) for $\sqrt{N}g_{31} = \sqrt{N}g_{32} = 50\gamma$ and $\Omega = 100\gamma$. (a) $\gamma t = 2.5$, (b) $\Delta = 500\gamma$. $\delta = 2000\gamma$ (thick red lines), $\delta = 1183\gamma$ (thin blue lines).

are for $\eta = 78.5\%$, and the light dashed lines are for ideal detection. It is seen that there exists a maximum value of gain and quantum correlation in accordance with previous experimental results, and the maximum value is found at larger detuning Δ for larger δ; this means that in order to achieve high squeezing in the Cs atom cell, large Δ is needed. Meanwhile, the window of gain spectrum becomes wider for larger δ. Figure 6(b) shows that the gain (solid lines) and the degree of quantum squeezing (dashed lines) increase with increasing t. Note that the higher the ground-state hyperfine splitting δ is, the lower the gain will be for the same interaction time. It gives an explanation of our experimental results that the high degree of squeezing is difficult to obtain; furthermore the improvement of squeezing can be found at higher Δ and with longer length of vapor cell. We note from Figs. 5 and 6 that the possibility of reaching 4.5 dB squeezing can be established in Cs atoms. However, in our experiment, lower than 3 dB squeezing is obtained; such a deviation might be caused by several factors of the Doppler broadening from thermal atoms at high temperature, vapor cell's transmission loss, self-focusing, laser frequency stability, and mechanical vibration of the system.

V. CONCLUSION

In this paper, we experimentally demonstrated the generation of quantum-correlated twin beams in a Cs atomic vapor cell, and established a theoretical framework of effective Hamiltonians for investigating the dependence of intensity-difference squeezing on the parameters of an atomic system. The difficulty of getting a high degree of twin beams in Cs atoms was revealed. Though the current experimentally achieved squeezing about 2.5 dB was not a promising value for further application, we can expect some improvement to be made via exploring other atomic levels, e.g., Zeeman sublevels in Cs atoms.

ACKNOWLEDGMENTS

This work was supported by National Basic Research Program of China (Grants No. 2010CB923102, No. 2012CB921603, and No. 2011CB922203), National Natural Science Foundation of China (Grants No. 11274210, No. 61308121, and No. 61108003), and the Project for Excellent Research Team of the National Natural Science Foundation of China (Grant No. 61121064).

[1] S. L. Braunstein and P. van Loock, Rev. Mod. Phys. **77**, 513 (2005).
[2] P. H. Souto Ribeiro, C. Schwob, A. Maître, and C. Fabre, Opt. Lett. **22**, 1893 (1997).
[3] J. Mertz, T. Debuisschert, A. Heidmann, C. Fabre, and E. Giacobiono, Opt. Lett. **16**, 1234 (1991).
[4] J. Gao, F. Cui, C. Xue, C. Xie, and K. Peng, Opt. Lett. **23**, 870 (1998).
[5] J. Brendel, N. Gisin, W. Tittel, and H. Zbinden, Phys. Rev. Lett. **82**, 2594 (1999).
[6] E. Brambilla, L. Caspani, O. Jedrkiewicz, L. A. Lugiato, and A. Gatti, Phys. Rev. A **77**, 053807 (2008).
[7] I. P. Degiovanni, M. Bondani, E. Puddu, A. Andreoni, and M. G. A. Paris, Phys. Rev. A **76**, 062309 (2007).
[8] V. Boyer, A. M. Marino, R. C. Pooser, and P. D. Lett, Science **321**, 544 (2008).
[9] V. Boyer, A. M. Marino, and P. D. Lett, Phys. Rev. Lett. **100**, 143601 (2008).
[10] N. Treps, U. Andersen, B. Buchler, P. K. Lam, A. Maître, H.-A. Bachor, and C. Fabre, Phys Rev. Lett. **88**, 203601 (2002).
[11] S. Reynaud, C. Fabre, and E. Giacobino, J. Opt. Soc. Am. B **4**,1520 (1987).
[12] A. S. Lane, M. D. Reid, and D. F. Walls, Phys. Rev. Lett. **60**, 1940 (1988).
[13] J. I. Cirac, P. Zoller, H. J. Kimble, and H. Mabuchi, Phys. Rev. Lett. **78**, 3221 (1997).
[14] C. W. Chou, H. de Riedmatten, D. Felinto, S. V. Polyakov, S. J. van Enk, and H. J. Kimble, Nature **438**, 828 (2005).
[15] M. Fleischhauer and M. D. Lukin, Phys. Rev. A **65**, 022314 (2002).
[16] L. M. Duan, M. Lukin, J. I. Cirac, and P. Zoller, Nature **414**, 413 (2001).
[17] C. H. van der Wal, M. D. Eisaman, A. André, R. L. Walsworth, D. F. Phillips, A. S. Zibrov, and M. D. Lukin, Science **301**, 196 (2003).
[18] V. Balić, D. A. Braje, P. Kolchin, G. Y. Yin, and S. E. Harris, Phys. Rev. Lett. **94**, 183601 (2005).
[19] A. Kuzmich, W. P. Bowen, A. D. Boozer, A. Boca, C. W. Chou, L.-M. Duan, and H. J. Kimble, Nature (London) **423**, 731 (2003).
[20] K.-J. Boller, A. Imamoğlu, and S. E. Harris, Phys. Rev. Lett. **66**, 2593 (1991).
[21] H. Schmidt and A. Imamogdlu, Opt. Lett. **21**, 1936 (1996).
[22] L. Deng and M. G. Payne, Phys. Rev. Lett. **91**, 243902 (2003).
[23] H. Kang, G. Hernandez, and Y. Zhu, Phys. Rev. A **70**, 061804(R) (2004).
[24] S. Du, E. Oh, J.-M. Wen, and M. H. Rubin, Phys. Rev. A **76**, 013803 (2007).
[25] D. A. Braje, V. Balić, S. Goda, G. Y. Yin, and S. E. Harris, Phys. Rev. Lett. **93**, 183601 (2004).
[26] C. F. McCormick, V. Boyer, E. Arimondo, and P. D. Lett, Opt. Lett. **32**, 178 (2007).
[27] C. F. McCormick, A. M. Marino, V. Boyer, and P. D. Lett, Phys. Rev. A **78**, 043816 (2008).
[28] A. M. Marino, R. C. Pooser, V. Boyer, and P. D. Lett, Nature **457**, 859 (2009).
[29] C. Liu, J. Jing, Z. Zhou, R. C. Pooser, F. Hudelist, L. Zhou, and W. Zhang, Opt. Lett. **36**, 2979 (2011).
[30] Q. Glorieux, L. Guidoni, S. Guibal, J.-P. Likforman, and T. Coudreau, Phys. Rev. A **84**, 053826 (2011).
[31] T. T. Grove, M. S. Shahriar, P. R. Hemmer, P. Kumar, V. S. Sudarshanam, and M. Cronin-Golomb, Opt. Lett. **22**, 769 (1997).
[32] Q. Glorieux, R. Dubessy, S. Guibal, L. Guidoni, J.-P. Likforman, T. Coudreau, and E. Arimondo, Phys. Rev. A **82**, 033819 (2010).
[33] M. Jasperse, L. D. Turner, and R. E. Scholten, Opt. Express **19**, 3765 (2011).
[34] S. Knappe, V. Shah, P. D. D. Schwindt, L. Hollberg, J. Kitching, L.-A. Liew, and J. Moreland, Appl. Phys. Lett. **85**, 1460 (2004).
[35] D. Pinotsi and A. Imamoglu, Phys. Rev. Lett. **100**, 093603 (2008).

[36] D. Höckel and O. Benson, Phys. Rev. Lett. **105**, 153605 (2010).
[37] J. X. Zhang, H. T. Zhou, D. W. Wang, and S. Y. Zhu, Phys. Rev. A **83**, 053841 (2011).
[38] J. X. Zhang, J. Cai, Y. F. Bai, J. R. Gao, and S. Y. Zhu, Phys. Rev. A **76**, 033814 (2007).
[39] Y. Li, D. H. Cai, R. Ma, D. Wang, J. R. Gao, and J. X. Zhang, Appl. Phys. B **109**, 189 (2012).
[40] W. R. Bosenberg, A. Drobshoff, J. I. Alexander, L. E. Myers, and R. L. Byer, Opt. Lett. **21**, 1336 (1996).
[41] D. Wang, L. Y. Hu, X. M. Pang, J. X. Zhang, and S. Y. Zhu, Phys. Rev. A **88**, 042314 (2013).